DOI: 10.15587/978-617-8360-09-2.CH5

Bogdana Gayvas, Bogdan Markovych,
Anatolii Dmytruk, Veronika Dmytruk

CHAPTER 5

ON THE ISSUES OF OPTIMIZATION AND REGULATION OF THE CONVECTIVE DRYING PROCESS OF MATERIALS IN DRYING UNITS

ABSTRACT

The Chapter presents the main approaches to optimizing and regulating the drying process of materials, taking into account the structural characteristics and operating principles of drying equipment. An essential factor in optimizing such processes is the consideration of the drying object and the mathematical methods used to describe drying problems. To this end, widely applied practical methods of mathematical modeling of capillary-porous and dispersed materials are analyzed, along with the specific features of models that describe heat and mass transfer in such materials.

Particular attention is given to the role of diffusion and thermo-diffusion mechanisms in moisture transfer regulation. Optimization strategies are developed using fundamental drying principles, where the Kirpichov criterion provides a quantitative assessment of moisture transport dynamics, while Nusselt numbers serve as key parameters for controlling temperature gradients and ensuring efficient moisture removal. Additionally, the Postnov criterion is used as a means of evaluating the balance between temperature gradients and moisture content distribution, helping to prevent excessive stress accumulation that may lead to cracking. The study further explores empirical relationships between these criteria and essential process parameters, including moisture content, temperature, and airflow velocity, to enhance drying efficiency and maintain structural integrity.

The study investigates the peculiarities of constructing mathematical models of non-isothermal moisture transfer and deformation during the drying of capillary-porous, dispersed, and fractal-structured materials from the perspective of continuum mechanics, mixture theory, and statistical approaches. This allows for the broadest possible range of model implementations, accounting for the anisotropy of thermomechanical properties, elastic and viscoelastic behavior, material shrinkage, and other relevant factors.

KEYWORDS

Mathematical modeling, drying, capillary-porous body, dispersed materials, gas-suspended state, fluidization, relative moisture content, stress, optimization, heat and mass transfer, deformation, anisotropy, numerical methods.

The effective resolution of several significant scientific and technical problems related to the drying processes of capillary-porous bodies requires consideration of the material's structure, real mechanisms of heat and moisture transfer depending on the drying method, the influence of kinetic and geometric characteristics of the body, and the control parameters of the drying agent. Additionally, these factors affect the stress-strain state and the stability of the body's shape. The preservation of material quality during the drying process is based on specific macroscopic physico-mathematical models of heat and mass transfer and necessitates efficient analytical and numerical methods for solving the corresponding boundary value problems of mathematical physics. These models are constructed using the fundamental principles of continuum mechanics and the thermodynamics of non-equilibrium processes.

However, capillary-porous bodies are multiphase and heterogeneous during the drying process. To represent multiphase characteristics approaches from mixture theory and methods from the mechanics of multi-velocity systems are utilized alongside capillary models of porous media and combined methods. These approaches incorporate capillary models for heat and mass transfer modeling while employing homogenization methods for solving mechanical problems, deriving physical relationships for the body as a whole based on specific assumptions about the temporal and spatial variations of the studied fields.

To account for the material's structure, the interaction of heat and mass transfer processes within the body, and the impact of heat and mass exchange between the body's surface and the drying agent on phase transition processes, methods of effective properties and stochastic approaches are applied.

5.1 FUNDAMENTALS OF HETEROGENEOUS MEDIA DESCRIPTION

In multiphase systems, structural effects and their changes, interphase interactions – particularly capillary effects – phase transitions, particle rotation, and collisions occur [1]. Colloidal mixtures occupy an intermediate position between heterogeneous and homogeneous mixtures. The solid particles in a dispersed mixture are referred to as dispersed, while the continuous carrier phase is called the dispersion medium.

The laws governing the motion of heterogeneous systems are essential, especially in processes involving a fixed granular layer through which a gas mixture is passed, processes with a granular layer suspended by a gas flow, and processes in a porous medium, which represents a heterogeneous system containing liquid or gas in its pores. When analyzing heterogeneous systems, it is assumed that the size of inclusions and inhomogeneities in the mixture is significantly larger than molecular-kinetic scales but smaller than the inhomogeneities at which the macroscopic or averaged parameters of the mixture change substantially.

These assumptions allow for the investigation of the behavior of individual inclusions and the processes occurring near them. This includes studies on heat exchange, phase transformations around and within particles, deformations within the particles or the skeleton of capillary-porous bodies, and the behavior of mixtures in channels, among other aspects. Most materials undergo drying in a dispersed state, which has led to the increasing application of various hydrodynamic modes of fluidized beds for drying.

In each continuum, distinct macroscopic parameters are defined, such as velocity, density, pressure, and temperature. The results of microprocess studies are incorporated into continuum equations through averaged parameters describing interphase interactions.

Homogeneous mixture.

In homogeneous mixtures (such as solutions and gas mixtures), the components interact at the molecular or atomic level, and their relative motion velocities are small. These velocities need to be considered only when determining the concentration of components. The diffusion approximation in mixture mechanics is associated with neglecting the dynamic and inertial effects of diffusion velocities.

The relative motion of components, described by diffusion velocities or diffusion fluxes, is determined by the diffusion mechanism, which establishes dependencies on concentration gradients, temperature gradients, and pressure gradients. In this approach, the inertia of the relative motion of the components is disregarded [2].

Model of a heterogeneous mixture.

Unlike homogeneous mixtures, liquid-solid suspensions (e.g., slurries, water-saturated soils, etc.) are described by a multi-velocity model that accounts for dynamic effects due to velocity mismatches between the components (phases). In a heterogeneous mixture, each phase occupies only a fraction of the total volume. Therefore, volume fractions of the mixture are used, along with specific densities, in addition to the apparent densities.

The phases exist as macroscopic entities relative to molecular dimensions. Consequently, the deformation of each phase, which determines its state and response, is associated not only with the displacement of external boundaries – described by the velocity field *v*, which may differ significantly from the mass-averaged velocity field *v* of the selected volume – but also with the displacement of interphase surfaces within the selected mixture volume.

For each phase, both the external deformation rate tensor and a set of tensors accounting for the displacement of the substance of phase *i* at interphase boundaries are considered. Thus, the true deformation rate of a phase is determined by the tensor: $e_i^{*kl} = e_i^{kl} + \sum_{j=1, j \neq i}^{m} e_{ij}^{*R}$. The determination of e_{ij}^{*R} is associated with considering the conditions of joint deformation and motion of the phases, as well as the structural properties of the medium's components. When strength effects are negligible, such as in gas-suspended states or in solid bodies under high pressures, the conditions for joint motion are simpler than in the general case. They reduce to equations defining phase volume fractions, pressure equality conditions between phases, or incompressibility conditions for one of the phases.

If the temperature T_i of each phase can be determined at any arbitrary point in the mixture, then, unlike the homogeneous case, the equations of state take the form: $\sigma_i^{kl} = \sigma_i^{kl}(\rho_i^0\ e_i^{0mp}, T_i, \chi_i^1, \ldots, \chi_i^r)$, $u_i = u_i(\rho_i^0, T_i, \chi_i^1, \ldots, \chi_i^r)$. These equations are defined not by the average, but by the true densities of the components ρ_i^0.

Additionally, the laws governing the relative motion of the phases become more complex, as this motion is influenced not only by diffusion processes but also by phase interactions at the macroscopic level. For example, in a gas-suspended state, the influence of interphase forces must be taken into account, including phase inertia, mass exchange, force interactions, and energy interactions.

When the relative motion processes are insignificant compared to the phase-averaged velocity, and the dynamic and inertial effects of this motion are small, a diffusion approximation can be applied to describe heterogeneous mixtures, with some modifications due to the presence of a suspended phase. A notable example of a non-inertial diffusion law is Darcy's filtration law: $\rho_i w_i = k\nabla P$.

To close the system of equations, barotropic-type state equations are used: $P = P_i = P_i(\rho_i^0)$. This approach is valid when the size of inclusions significantly exceeds molecular dimensions.

Motion of a heterogeneous medium with phase transitions.

The momentum exchange between phase *i* and phase *j* per unit time and per unit volume is expressed as $P_{ji} = -P_{ij} = R_{ji} v_{ji,}$ $(i, j = 1,..m)$, where R_{ji} is the interphase force per unit volume due to friction, pressure, and adhesion between phases, and v_{ji} represents the velocity or momentum of mass undergoing transformation from phase *j* to phase *i.*

If each phase is assumed to be homogeneous up to the phase boundary surface within an elementary volume of the mixture, and if the energy of each component is proportional to its mass, then the influence of the interfacial layer – on the order of the molecular interaction radius (10^{-9} m) – can be neglected. This assumption requires that all inclusion sizes be significantly larger than the thickness of this layer. Furthermore, the energy equation should not account for small-scale flow effects, such as micro-scale chaotic motion of inclusions. Under these conditions, the kinetic energy of the mixture, when represented homogeneously, is additive over the mass of the phases. The introduction of phase temperatures is linked to the hypothesis of local equilibrium.

Using averaging methods, the momentum equations, heat flux equations for phases, and energy equations for pulsational (small-scale) motion can be derived [26, 30].

Porous medium saturated with liquid or gas.

In a two-phase mixture of a porous solid phase with liquid or gas, the total stress is determined by the fictitious stresses and the pressure exerted by the liquid or gas. Fictitious stresses are defined through directly measurable quantities and pressure and interpreted as part of the average stress tensor in the solid phase or skeleton. These stresses are caused by an independent force transmission mechanism through contacts between the grains, rather than by the liquid. The strength properties of the solid phase manifest in the fictitious stress tensor.

Studies [4, 5] have classified drying objects. A. Lykov divided all solid wet materials into three groups: capillary-porous, colloidal, and capillary-porous colloidal materials. Capillary-porous colloidal materials are those in which liquid exhibits different forms of bonding, which are characteristic of both capillary-porous and colloidal bodies. In particular, in capillary-porous bodies, the liquid is bound by capillary forces. Upon dehydration, capillary-porous bodies become brittle. They exhibit low compressibility and high liquid absorption capacity. Capillary forces significantly exceed gravitational forces.

Colloidal materials are those in which moisture is primarily bound by adsorption and osmotic forces. When dried, colloidal bodies contract with maintaining elasticity [2]. When moistened, they absorb liquids that are most similar in polarity. These materials are quasi-capillary-porous bodies, where molecular sizes are comparable to microcapillary dimensions.

B. Sazhin [6] classified dispersed materials into four groups based on the decreasing critical pore radius: greater than 100 nm; from 100 to 6 nm; from 6 to 2 nm; 2 nm or less. Additionally, he introduced subgroups and classes considering the particle size of the material, its adhesion-cohesion properties, and drying duration.

A two-phase dispersed mixture that contains dispersed particles of uniform shape and size within an elementary macro volume is called monodisperse. If the particles vary in size, the mixture is polydisperse. The carrier phase is a spatially connected volume (the dispersion medium).

An essential characteristic of convective drying is the gas and vapor pressure in both the drying agent and the material being dried.

Models of corpuscular structure.

Dispersion is a thermodynamic characteristic of a system that determines the magnitude of the phase interface. The degree of dispersion is the degree of fragmentation of the substance in the dispersed phase, which is inversely proportional to the particle size $s = 1/l$, where l is the linear dimension that determines the particle size. L. Frevel [7] studied the method of forming regular packings composed of identical spheres. The distance between spheres varied from $\sqrt{3}R$, corresponding to the densest packing, to ρ_M, corresponding to the vertical alignment of layer centers directly above one another. The porosity ε in such packings varies from 0.2595 to 0.3954, and the coordination number for the densest packing equals 8.

K. Schlichter [2] studied another method of forming regular packings in the form of layers. The centers of the spheres were arranged at the nodes of rhombohedral lattices defined by the acute angle ω of the rhombus, with vertices at the centers of adjacent layers. An angle of $\omega = 60°$ corresponds to the densest packing with $\varepsilon = 0.2595$, while $\omega = 90°$ corresponds to simple cubic packing with $\varepsilon = 0.4764$. The coordination number for such packing is $N = 12$.

If regions around the voids are cut out such that the cutting planes pass through the narrowest cross-sections of pore necks, the porous body is divided into elementary cells – polyhedra. An elementary pore in such a cell represents a cavity bounded by spherical surfaces with several necks connecting it to other elementary pores. In cubic packing, the elementary pore cavity is bounded by eight spheres and connected to six square-shaped necks leading to neighboring cavities.

The sizes of elementary pores in framework packings are characterized by the radius ρ_{rop} of the sphere inscribed in the cavity and the equivalent radius ρ_{rop} of the circle inscribed in the neck.

According to V. Karnaukhov, for framework packings: $\rho_{3>@} \approx 0,45\dfrac{\varepsilon}{1-\varepsilon}R$. The shape and sizes of pores in random sphere packings vary, but their qualitative appearance is similar to elementary pores in regular packings. The specific surface area of particles is given by: $s_y = S/V_M$, where S and V_M are the surface area and volume of the particles in the material.

Drying of natural organic materials.

The process is accompanied by structural changes, physicochemical transformations, endothermic and exothermic reactions. Variations between isosteric and calorimetric values of specific heat of evaporation for starch and cellulose have been observed. These variations are caused by changes in the configurational entropy of solid components and the entropy of mixing due to interactions between solvent molecules (water) and macromolecules of high-molecular substances. However, during the removal of capillary and adsorbed moisture, an increase in the specific heat of evaporation is observed by only 3–5 % and 20 % relative to the evaporation heat of bulk liquid, respectively.

At low moisture contents, individual water molecules reside in micropores, comparable in size to the sorbate molecule, and interact via hydrogen bonds with the polar functional groups of the sorbent. If the pores are larger and not fully filled, translational motion of sorbate molecules may occur inside them. As the pores fill, mobility decreases. At high moisture contents, the material swells, and pore sizes increase. Water molecules in such conditions are more mobile, and as intermediate and macropores fill, their mobility approaches that of ordinary water molecules. The swelling process is analogous to the dissolution of water in a high-molecular substance. With increasing moisture content, water molecule clusters merge and form a continuous phase within the sorbent, defining the physical properties of the sorbate, which become similar to those of a typical liquid.

The sorption isotherm on swollen colloidal materials is described as $1/W = n\ln(P_s/P) + a$, where W is the moisture content, P_s/P is the relative vapor pressures of the sorbate, and a, p are constants. The primary indicator characterizing a material as a drying object is moisture resistance, which determines the limit of residual moisture in the dehydration process. Living cells exhibit high moisture sensitivity. Their physicochemical properties and responses to dehydration conditions vary significantly. Consequently, no consistent pattern has been found linking residual moisture to microbial cell viability, often resulting in a final product with a low count of viable cells.

When biological systems are dried, they enter a state of dry anabiosis, in which vital processes are suppressed, but a lethal state does not occur. Upon restoration of favorable conditions, normal metabolic processes can resume. Water acts as a regulator of essential metabolic processes between the cell and its external environment [7, 8].

Experimental data reveal a pattern for vegetative microbial cultures of various origins, showing a sharp loss of microbial cell viability within the moisture content range of 50–80 %. The effect of residual moisture on microbial viability exhibits a stepwise nature, where the primary lethal factor is the sudden rupture of the cell membrane. The critical moisture content, corresponding to a drastic change in microbial viability, coincides with the maximum hygroscopic moisture content, and the viability decline region aligns with the sorption isotherm segment where moisture is primarily capillary-bound.

For a given relative air humidity, the average capillary radius is determined using the Thomson equation:

$$\overline{r} = \frac{2\rho_v \sigma \cos\Theta}{\rho_L P \ln(1/\varphi)}.$$

Thus, for $\varphi = 0.96$, the mean capillary radius is $r = 10^{-5}$ cm. In this case, the capillary rise height is $h = 150$ m, and the pressure of such a column is approximately 1.5 MPa. If the capillary height is less than h, a negative pressure is generated within the capillary, causing deformation of the elastic body skeleton (cell membranes). Liquid under negative pressure exists in an unstable metastable state. However, a metastable phase can persist indefinitely under unchanged thermodynamic conditions, which is associated with the stationary state of a dehydrated biological system – anabiosis. A necessary condition for anabiosis is the presence of a metastable liquid film around a living cell, forming part of the capillary-porous body structure.

In work [9], a model for unsteady processes of a single-component liquid was proposed, accounting for the mutual influence of vapor pressure, liquid pressure (determined by capillary and surface forces), temperature on phase mass exchange intensity, thermocapillary flows, and the conditions for mechanical and dynamic equilibrium of thin liquid layers on curved phase interfaces.

Material permeability.

In work [10], a dependence of the permeability coefficient on the effective pore size was obtained based on the differential pore characteristics of the material and Darcy's law for different moisture contents. The permeability of dry materials is expressed through the linear dependence of gas flow through a porous medium on the gas pressure gradient.

As the liquid is removed from a material initially saturated to its maximum moisture capacity, it exits the largest pores and then the smaller ones. During this process, the effective porosity of the material and the permeability coefficient change. By maintaining a constant pressure difference under filtration conditions, the volumetric airflow rate J_0 can be measured. Given the known sample thickness, filtering surface, and viscosity of the absorbed liquid, the material's permeability can be calculated as a function of the minimum diameter of open pores.

Since the applied air pressure compensates for the capillary pressure of the liquid in the material's pores, the minimum diameter of open pores is determined using Laplace's equation. A stepwise increase in pressure difference leads to the sequential displacement of liquid from progressively smaller pores, thereby altering the permeability coefficient. To determine the material's permeability and the minimum diameter of open pores, the moisture content of the sample must be measured at each pressure difference increment. Studies show that the effective radius of open pores significantly influences the permeability coefficient.

Drying process and product quality.

The quality of the final product obtained through drying is determined by the heat-moisture conditions and the mechanism of heat and mass transfer. Studying diffusion and thermodiffusion processes enables a better understanding of substance movement within the material, the identification of effective ways to control mass transfer mechanisms, and the development of new drying technologies to enhance product quality.

If liquid moisture diffusion occurs during drying, water-soluble substances accumulate on the surface. In contrast, when vapor-phase moisture diffusion dominates, water-soluble components remain within the material.

Suspended-state grain drying.

The method of drying grain in a suspended state involves a continuous alternation between heating and cooling processes. In intermittent drying, the surface layer of the grain cools more than the inner layers. In such cases, thermomoisture conductivity supports moisture transfer, and the heat flux aligns with the moisture flux. Moisture evaporation starts from the surface, causing water-soluble nutrients to remain near the surface and close to the germ, promoting its growth and improving the seed quality.

During drying, materials undergo shrinkage. High-quality material maintains uniform shrinkage throughout its thickness. Significant variations in moisture content and temperature during drying result in volumetric stress-strain states that exceed permissible limits, leading to cracking or complete structural failure. Materials may warp or develop pores. The surface with lower moisture content contracts more, causing the sample to warp toward the drier side. Ideally, the moisture transfer mechanism should ensure equal moisture removal rates from both surfaces.

Temperature gradients drive moisture movement inside the material. The moisture flux toward the surface decreases by an amount proportional to the thermodiffusion-induced moisture flux, which opposes the movement of moisture from the central layers to the surface. Thermodiffusion reduces the moisture gradient, decreases moisture transfer rates, and limits the accumulation of water-soluble substances on the surface. Changes in the temperature gradient's direction alter the material's physicochemical and biochemical properties. To retain water-soluble substances within the material, the most intense evaporation should occur inside the material rather than at the surface.

The temperature gradient increases with airflow velocity. In thick materials, an increase in temperature gradient results in a moisture content gradient, leading to internal stresses and crack formation.

Steam-heat treatment drying.

In steam-heat drying, saturated steam is used as the heat carrier. Heat is transferred from the steam-air mixture to the solidifying material through convection. A temperature gradient is established in the material, generating internal stresses. Since the surface temperature is lower than that of the steam-air mixture, a condensate film forms on the surface, and moisture migrates from the surface layers to the center, leading to material reabsorption of moisture. The hydration reaction occurring during this process can cause the material's temperature to exceed that of the surrounding environment. Intense evaporation at high moisture levels results in directed pore formation.

To control moisture transfer, it is essential to establish the relationship between diffusion and thermodiffusion coefficients with moisture content and temperature, particularly using stationary and non-stationary mass transfer methods.

Models based on continuum mechanics.

Changes in the volume and shape of solid porous bodies during drying in the absence of external forces indicate the emergence and development of a stress-strain state caused by moisture-thermal effects [15]. Colloidal materials undergo dimensional changes during drying. The removal of moisture from the material requires energy, which corresponds to breaking the bonds between the moisture and the material.

Physico-mechanical bound moisture is present in large capillaries and on the external surface of the material. Removing this moisture requires energy equal to the heat of vaporization. Physico-chemical bound moisture is retained on the internal surface of pores by adsorption forces. The amount of adsorbed moisture depends on the temperature and humidity of the external environment.

As temperature increases and moisture content in the body decreases, two opposing processes occur: thermal expansion and contraction, which are governed by the physical properties of the material. These opposing deformations restrict each other, leading to the formation of nonstationary stresses, which can exceed the strength limit, resulting in crack formation and propagation.

Studying the stress-strain state in drying kinetics and comparing stress values with material strength characteristics allows optimization of drying processes based on strength parameters. In work [15], a mathematical drying model was developed that accounts for the stress-strain state of the material based on non-equilibrium thermodynamics and continuum mechanics.

It is assumed that the wet body is isotropic and undergoes small elastic, nonlinear elastic, and plastic deformations, where linear deformation theory holds. The capillary-porous body is considered as a local superposition of a solid porous or granular component and a fluid phase (in liquid and vapor states) filling the pores. During drying, the body is treated as a heterogeneous non-equilibrium system that exchanges energy and mass with the surrounding environment.

The principle of local equilibrium in non-equilibrium thermodynamics enables the description of the system using equilibrium state parameters. During drying, the temperature, volume, and composition of the system change. The composition changes only due to phase transitions of the liquid and vapor removal.

If evaporation occurs at temperature T, evaporation of liquid in the pores occurs, an excess vapor pressure arises in the system $p = P - P_0$, where P_0 is the barometric pressure. This excess pressure causes tensile deformation p / E_0, which leads to convective mass transfer, alters the phase transition temperature, affects the mass transfer intensity, and influences material compression. At different drying stages, the intensities of these components vary, and the resulting deformation may manifest as either tensile or compressive deformation.

A mathematical model of capillary-porous material drying is formulated, including:

1. Equation of state.
2. Diffusion-convective mass transport equation.
3. Momentum equation.
4. Heat conduction equation.
5. Compatibility conditions for deformations.

A closed system of nonlinear equations describes the time-dependent processes of heat and mass transfer and deformation, considering the dependence of thermophysical, heat and mass transfer, and physico-mechanical properties on temperature and moisture content.

These equations, with initial and boundary conditions, define a nonstationary drying problem and establish the interrelation between heat and mass transfer and the stress-strain state.

In drying process formulation in displacements, the diffusion-convective mass transport equations in displacements are used along with the corresponding heat and mass exchange boundary conditions and mechanical boundary conditions ensuring deformation compatibility.

For drying technology applications, interest lies in the deformations and stresses induced by moisture-thermal effects. It is shown that in transport equations, the mechanical coupling terms can be omitted, while in equilibrium equations, hydro-barothermal field variations can be disregarded.

The continuum mechanics approach to studying the stress-strain state is detailed in work [16].

Stress and deformation relations.

The stresses induced during drying lead to elastic-plastic deformations, which are determined by the relationship between the strain tensor ε_{ij} and the stress tensor σ_{ij}:

$$\sigma_{ij} = f(\varepsilon_{ij}).$$

Since drying-induced stresses have a negligible effect on the excess vapor-air mixture pressure within the body, the coupling effect is insignificant in problems concerning moisture-thermal stresses in drying materials.

In the heat conduction equation, the mechanical coupling terms can be neglected, and in the momentum equation, the inertial term can be omitted. The interaction between heat and mass transfer and the stress-strain state is also negligible in most cases.

On the boundary surface, the components of internal stresses must equal the external surface forces. In many drying cases, volume and surface force loads can be neglected.

As a result of heat and mass transfer through the material thickness, nonstationary temperature, moisture content, and pressure fields develop, which are determined from the heat and mass transfer equations.

To solve the drying problem, six stress tensor components σ_{ij} must be determined, satisfying:

a) six equilibrium equations;

b) deformation compatibility equations;

c) boundary conditions;

d) these relationships enable a comprehensive analysis of moisture-thermal stresses and deformations in drying processes.

Models based on mixture theory.

In works [17, 18], the laws of non-equilibrium thermodynamics were applied to a three-phase medium consisting of a solid skeleton, liquid, and vapor-air mixture in a porous deformable system to analyze interphase interaction forces, considering phase transitions.

The porous body was treated as a thermodynamic system comprising solid, liquid, and gaseous phases. The solid particles were tightly packed into either a granular skeleton or a capillary-porous body. Initially, the pores were filled with moisture and air. Under the influence of external heat sources and pressure differences between the pores and the surrounding environment, interconnected heat and mass transfer and deformation processes occurred.

It was assumed that the gaseous phase is homogeneous. Due to capillary forces, pressure differences in the capillaries, and chemical activity of liquid and gaseous phase particles, chemical transformations and phase transitions of the components may occur in the capillaries.

Particles of the same chemical species, when in different aggregate states, exhibit different diffusion, filtration, and thermal conductivity coefficients. In a p-component three-phase system with chemically active elements, phase transitions of the components can occur.

Chemical transformation can be considered as a complex interaction of thermal, mechanical, mass, and electrical processes among the subsystems.

The mass balance equations for each component and the law of conservation of total energy of the system are postulated. Balance relations for the momentum of the total system mass, considering chemical transformations, potential, kinetic, and internal energies, entropy, and the Gibbs equation for free energy are obtained.

Assuming that the kinetic potential is a function of thermodynamic forces, kinetic relations for the thermodynamic system are derived [17, 18].

Thus, a complete nonlinear system of equations for the model is constructed, including:

1) the coupled heat conduction equation;

2) the equation of state (expressing the dependence of entropy, the total stress tensor, and chemical potential on temperature T, $\varepsilon_{\alpha\beta}$, $C_k^{(j)}$;

3) equations for liquid and gas phase pressures;

4) the equation for the density of saturated vapor;

5) mass balance equations for the skeleton, air, vapor, and liquid;

6) relations for the liquid, vapor, and air fluxes in terms of gradients T, $\varepsilon_{\alpha\beta}$, $C_k^{(j)}$;

7) invariants for the volume-averaged mixture related to skeleton dilation due to concentration differences;

8) the compatibility equation;

9) the momentum balance equation for the skeleton;

10) expressions for the components of the fictitious stress tensor;

11) the total stress tensor as a function of fictitious stresses and the stress tensor of the liquid and gas phases taking into account the viscosity effects;

12) the difference in pressure between the carrier and solid phases due to mechanical strength;

13) relations for volume-averaged velocities and skeleton deformations.

Application to engineering problems of conductive drying.

Based on this model, the problem of conductive drying of a porous layer is formulated as follows:

A thin plane plate with surface area S and thickness h_w is exposed to an external heat flux $q_e(t)$ on one side. The plate has density ρ_w and specific heat capacity c_w. A moisture-saturated capillary-porous material of thickness l is placed on the plate. The material has the porosity Π, density ρ_0^0, specific heat capacity c_0, thermal conductivity coefficient in the dry state λ_0. From the exposed surface of the capillary-porous material, liquid evaporates into a cavity with volume V and depth V/S. The thermally insulated cavity has an opening, through which the vapor-air mixture escapes into the ambient environment at pressure P_e. Heating of the material induces filtration flow of both liquid and gas. The liquid flow is driven by the gradients of relative saturation α (the volume fraction of liquid in the pores), temperature T, and vapor-air mixture pressure P. The vapor and air fluxes are governed by pressure and mass concentration gradients of vapor in the mixture. The relative permeabilities of liquid and gas are proportional to their respective saturations. Appropriate initial and boundary conditions are formulated.

A model of convective-thermal drying of a layer in a drying system, considering the movement of the phase transition boundary, has also been developed.

In work [20], the drying problem was formulated for a non-stationary thermal regime of the drying agent in a drying system. The use of time-varying thermal regimes during drying can significantly reduce energy consumption and improve material quality.

When the temperature of the drying agent decreases, the temperature of the material's surface layers also decreases, creating an additional temperature gradient, which serves as a driving force for moisture migration within the material. This leads to an increase in relative humidity and moisture treatment of the material surface, reducing internal stresses.

The timing and duration of heat-moisture treatment are critical for different materials. Therefore, it is necessary to develop methods for:

a) investigating heat and mass transfer processes;

b) diagnosing the stress-strain state of materials;

c) determining optimal drying agent parameters based on diagnostic results;

d) formulation of the drying problem for a layer under a time-varying thermal regime.

To assess the influence of a time-dependent thermal regime in the drying system, the drying process is formulated for a layer $(-L \leq z \leq L)$, where moisture removal occurs through its surfaces under the influence of a convective-thermal non-stationary flow of the drying agent.

The problem is reduced to solving the Stefan problem, which includes the following system of equations in the dried zone:

1. Energy equation.
2. Mass transfer equation for the vapor-air mixture.

3. State equation for the binary vapor-air mixture.
4. Energy balance equation at the moving phase transition boundary.
5. Linearized state equation at the moving phase transition boundary $z = L_m$.
6. Equation of motion for the phase interface.
7. The boundary conditions at $z = L$ express heat exchange between the material surface and the drying agent by the Newton's law.

At the phase transition boundary $z = L_m$, the transition temperature T_m is unknown and depends on the pressure P_n of the saturated vapor $(T_m = f(P_n))$ is to be determined; the time-dependent temperature of the drying agent is represented as a Fourier series expansion.

The solution algorithm was validated using a wood drying model (pine). The problem was reduced to solving the Stefan-Maxwell system of equations. Given a specified vapor flux across the thickness, the relationship between the phase transition coordinate and time was constructed. By solving the heat and mass transfer equations under a non-stationary drying agent regime with three-stage temperature control [20, 21], it was shown that as the mass transfer coefficient and temperature increase, and as the vapor density decreases, the relative humidity of the layer decreases; numerical results demonstrate parabolic dependencies of relative saturation over time and linear dependencies on changes in mass transfer coefficients.

The temperature distribution across the material thickness was determined as a function of dimensionless coordinate $\bar{z}$ and phase transition coordinate $\bar{z}_m$; the phase transition temperature variation over time was analyzed; the change in the phase transition coordinate over time was evaluated in relation to the relative saturation of the drying agent; the relationship between drying time and the width of the dried zone z_m was studied as a function of the heat transfer coefficient, mass transfer coefficient, permeability, diffusion, and average temperature.

It was shown that in a non-stationary regime, drying time depends both on the equation of state at the phase transition boundary and the heat and mass transfer coefficients. In a gentle drying regime, the process can be controlled by increasing or decreasing airflow speed via heat or mass transfer coefficients; adjusting the drying agent humidity; modifying the temperature change intervals of the drying agent using the control function expansion coefficients $u(\tau)$. The study demonstrated the possibility of selecting and minimizing optimal drying criteria [17–21].

The drying of dispersed materials in a suspended state was studied in [22]. The external heat and mass transfer process was analyzed based on the simultaneous consideration of the equations of motion and continuity for the drying agent flow and the convective-diffusive transfer of vapor and heat in the moving drying agent.

Experimental data on the intensity of external heat and mass transfer were presented as dependencies between similarity criteria derived from the governing equations and corresponding uniqueness conditions. The mass transfer coefficient appears in the Nusselt criterion, whose value is a function of the Reynolds and Prandtl numbers.

For forced airflow along a wet surface, the criterion equations for heat and mass transfer were provided based on experimental studies on the intensity of heat and mass exchange between the drying agent and the material, whose surface remains moist due to moisture supply from internal zones of the material.

Further, moisture undergoes phase transformation into vapor within the internal zones, causing the external surface temperature to increase and the heat and mass transfer coefficients to change. The variation in heat transfer coefficient due to decreasing moisture content was accounted for by the ratio of moisture content u to the critical value u_{kr}, at which the constant drying rate period ends, and the surface ceases to be wetted. An approximate formula was derived, incorporating the contributions of the frontal and rear sections of a spherical body in mass transfer.

It should be noted that the equations of motion for the drying medium are nonlinear, and for the numerical implementation of velocity, an alternative approach was developed in [23] through the phase state diagram of an infiltrated dispersed medium. This diagram includes not only the stationary bed and the boiling layer but also vertical pneumatic transport and the circulating fluidized bed. Expressions were derived for calculating an important characteristic of flow systems – the transport velocity; the critical point on the phase diagram was identified, which determines the velocity at the onset of fluidization.

The heat and mass transfer in a dispersed medium were studied in [24] as occurring in a homogeneous continuum or in multiple coexisting homogeneous continua within each point in space without considering microscopic transport phenomena near individual particles. Macroscopic heat or mass conservation equations were formulated for a continuous medium containing dispersed phase particles, neglecting the effect of random fluctuations of the medium and particles on the transport processes.

5.2 STATISTICAL METHODS FOR STUDYING THE DRYING OF CAPILLARY-POROUS BODIES

In works [25, 26], the problem of random pulsations in a coarse-disperse fluidized bed was formulated. Additionally, the problem of convective thermal conductivity or diffusion near an individual particle was posed. The problem was solved for low Péclet numbers, which characterize heat and mass transfer in the vicinity of an individual particle. It was assumed that the spatial scale L of temperature fields or impurity concentration in a dispersed system is significantly larger than the internal structure scale l of the system, such as the distance between neighboring particles. The dispersed system was considered as a superposition of coexisting continua, each characterized by its own average velocity and temperature. The variations of these quantities were described by averaged conservation equations. A system of conservation equations for mass, heat, momentum, and angular momentum of continua was developed, simulating the phases of a monodisperse suspension. If the phases of the dispersed medium are stationary, these equations describe transport processes in composite granular materials.

Using the mass conservation equations of the phases, a model was derived in which the dispersed medium is considered a superposition of two continua, each having different velocities and temperatures. The equations contain unknown variables, such as concentration and temperature, averaged over the ensemble of particles. The problem of determining these variables in the form of functions or functionals of unknown variables and physical parameters is analogous to the problem of obtaining rheological equations of state for suspensions.

Averaged equations describing heat transfer in the continuous phase near a selected particle were formulated. Their solution allows for the calculation of the average temperature and heat flux on the particle surface. In the ensemble averaging process, it was assumed that particle placement is random and that the correlation weakening condition holds. This condition states that conditional averages, obtained by averaging over the particle distribution function, given that a certain fixed point is occupied by the center of a test particle, asymptotically approach the corresponding unconditional averages as the distance from this point increases.

Furthermore, the average temperature of the continuous phase at a given point approximately coincides with the value obtained by averaging the temperature only over those configurations in which the presence of a particle center at that point would be possible. By analyzing integral sums and neglecting terms quadratic in random deviations of local values from their averages, a differential heat transfer equation was derived for both the continuous and dispersed phases on average. The heat transfer in the continuous phase was represented as transport in a hypothetical medium that fills the entire space and contains distributed heat sources. The equation describing heat transfer near a particle with its center at $r=0$ was obtained similarly to the equation for the continuous phase, assuming conditional averaging only over configurations of all other particles that are compatible with the presence of a particle center at a fixed point. In such averaging, terms quadratic in fluctuations of values relative to their mean were neglected; a heat transfer equation was obtained in a coordinate system associated with the center of a particle in the continuous phase. The heat transfer inside a test particle was described, considering its rotation. On the surface at $r=a$ of the test particle, continuity conditions for temperature and heat flux were imposed, defining the interaction between the particle and the continuous phase, which closes the heat conduction problem near the test particle.

The evaporation or condensation of moisture is accompanied by a sudden absorption or release of latent heat of vaporization, which is determined at the normal boiling temperature according to Trouton's rule $r_{boil} = 88T_{boil}$, since from the Clapeyron-Clausius equation $dp/dT = r/T\Delta v$, where dp/dT is the derivative of pressure with respect to temperature, which is determined from the phase equilibrium curve. If the phase transition data are missing, $r_{boil} = (RT_{kp}T_{boil}\ln P_{kp})/(T_{kp} - T_{boil})$ is put.

The structure of a body is influenced by the liquid contained within the porous medium. Swelling is a specific case of structural deformation caused by the interaction of the liquid with the material. In the absence of specific interactions between the body and the liquid, swelling pressure P_{swel} is proportional to the surface tension of the liquid.

To describe the distribution of phases within a porous medium, it is necessary to apply structural models of porous media [30]. Since real porous materials possess irregular and random structures, only stochastic structural models can claim adequacy. The pore space is represented as a statistical ensemble of interconnected structural elements (pores), whose properties follow certain probabilistic laws.

In the elementary physical volume of the medium, a specific porous medium model must be selected. The most suitable statistical model should accurately describe the structure. To determine the effective transport coefficients for each phase, their interconnections as functions of macroscopic variables, the conditions governing the process within an individual pore, and the geometric characteristics of the porous structure, a key factor is the choice of an averaging method, which is determined by the selected porous medium model.

The principle of local equilibrium is applied to determine the characteristics of phase distribution. This principle considers the process in an elementary physical volume as occurring in an unbounded porous medium, neglecting transport phenomena and accounting only for the conditions of interphase boundary formation under capillary dynamic equilibrium between the phases. The distribution of phases in the pore space is governed by pressure differences between phases and capillary properties, considering electrochemical transformations, if present.

The statistical analysis of liquid and gas distribution in hydrophilic porous media is based on representing the pore space as a network of variable cross-section channels, forming a stochastic spatial lattice with a specific coordination number. This representation reduces the problem of liquid and gas distribution to that of the mutual arrangement of liquid-filled and gas-filled pores in a random lattice with certain statistical properties.

During drying, the gas phase in the pore space forms three characteristic configurations:

a) a connected system of gas-filled pores that extends to the external surface;

b) a two-phase system consisting of isolated liquid inclusions trapped by gas;

c) a liquid-filled pore system.

For each specific porous structure, there exists a critical moisture content at which the connectivity of the liquid phase is completely disrupted, and all moisture is localized in isolated inclusions. The critical moisture content is a structural characteristic of the porous medium and can be used for comparative analysis of different porous structures.

The connectivity factor plays a key role in transport processes. The transport of any substance through either the gas or liquid phase is only possible within a connected network of gas (or liquid) pores, some of which are dead-end pores blocked by liquid (or gas) at one end. If a given pore belongs to an isolated inclusion, long-range transport is impossible. In the case of gas-filled pores, moisture transport occurs through: convection, vapor diffusion in the vapor-air mixture, film flow driven by the disjoining pressure gradient. As the moisture content changes during drying, the mechanisms of transport also change.

The mutual phase distribution in the pore space determines the effective transport coefficients for each phase and the interphase surface areas. The capillary forces are responsible for the distribution of phases. The liquid content in a porous body changes through evaporation and capillary absorption. In a capillary-porous body, vapor, filtration, and film mechanisms of moisture transfer operate, aiding in the establishment of capillary equilibrium.

The vapor mechanism follows the sequence: evaporation → vapor transport through the vapor-gas phase → condensation. The filtration mechanism occurs due to liquid flow under the capillary pressure gradient. During evaporation, the meniscus recedes only in a wide capillary, while in a narrow capillary, the recession begins only after the entire wide capillary has been dehydrated. Additionally, the volume of liquid evaporated from the narrow capillary is immediately replenished at the rate of evaporation by liquid from the wide capillary.

It can be lowered below the equalizing mechanisms' rate by artificially reducing the evaporation rate through external drying conditions. For example, reducing the external moisture transfer rate increases the moisture content, leading to a nearly uniform moisture distribution across the thickness of the porous body. Non-uniform moisture distribution causes undesirable deformation of porous materials.

Experimental data confirm that the distribution of pore volumes governs the equilibrium distribution of liquid within a porous body according to capillary pressures P^k and the influence of the temperature gradient on the moisture content gradient in the porous body. During drying, the mutual phase distribution is established through the interaction of two factors: the transition of one phase into another and the redistribution of phases in the porous material due to differences in capillary properties.

The control of heat and mass transfer processes in heterogeneous, fluidized, and vibro-circulating media has been extensively studied in works [23–29].

In the monograph [30], it is shown that during the drying process, three distinct zones are formed: the outer gas zone, where all pores are completely dried, and the gas distribution across the thickness is nearly uniform; the intermediate two-phase zone, where both dried pores and liquid-filled pores coexist; the inner liquid zone, where all pores remain filled with liquid. If the removal of vapor from the evaporation zone is rapid, and capillary inflow and recondensation cannot sufficiently replenish moisture in the dried pores near the surface, the two-phase zone disappears, leading to the formation of a spatial front inside the material. This front separates the liquid and gas zones and gradually moves deeper into the material. Conversely, if capillary inflow and recondensation are effective, but vapor removal is hindered, the phase boundary follows pores of a specific radius – one that depends on the amount of liquid present but not on spatial coordinates. In this case, the two-phase zone extends throughout the entire volume.

During evaporation, the connected liquid system undergoes fragmentation. Once a critical threshold is reached, the liquid phase connectivity breaks within the elementary volume of the porous medium. The connectivity of the liquid phase plays a key role in the mechanism of capillary moisture transfer. The redistribution of moisture in disconnected inclusions occurs through capillary recondensation. In diffusive or migratory transport within a connected liquid system, provided that this system remains connected to the outer surface, the effective diffusion or electrical conductivity coefficients depend on the amount of connected liquid. If liquid-phase transport becomes impossible due to the loss of connectivity at moisture content $u < u_{kr}$, it leads to a non-uniform concentration of liquid during evaporation. The connected liquid pore system is also heterogeneous in terms of transport processes due to the presence of dead-end pores – pores that are blocked by gas at one end.

Model of intersecting variable-section capillaries.

If pores are represented as circular cylinders with a radius r that varies along their length and does not intersect, then the serial model of the porous medium is applied. The liquid-gas interface at any given time is located within the critical pore and moves deeper into the material during evaporation. Pores with a radius larger than the critical value are referred to as supercritical pores. These supercritical pores can branch, which facilitates gas penetration into the porous medium.

Random process model.

A randomly selected supercritical pore located at the surface of the material $(y=0)$ can, through branching and blocking, generate s supercritical pores with probability $p_s(y)$.

The pattern of pore filling with vapor depends on the relationship between the probabilities of blocking λ and branching v. If $\lambda > v$, the probability of blocking a supercritical pore near the surface is given by $p_{s=0}(y) = F(y,o)$. To determine λ and v, it is necessary to define the type of random process governing the radius variation along the pore length.

Random walk model.

In a purely random process, the blocking probability does not depend on the pore radius. However, in reality, the blocking probability of a supercritical pore depends on its radius. Thus, in the random walk model, the blocking process of supercritical pores occurs stepwise: evaporation begins in the widest pores, then progresses to narrower supercritical pores, these pores transition to the subcritical class with higher probability as their radius decreases. This process resembles a random walk in the radius space of pores.

Serial model.

In [31], a numerical solution to the two-dimensional problem of non-isothermal moisture transport in an anisotropic wood structure under convective drying was obtained by the serial model. Based on elasticity theory, internal thermohygroscopic stresses were determined.

The values for elastic modulus and strength limit were taken from the formulas derived by G. Shubin [32] for pine wood. The study showed that at the beginning of the drying process, internal stresses in the surface zone increase and later decrease. A stress drop was observed after the moisture content of the inner zone fell below the fiber saturation point, estimated at 25 %. The appearance of significant residual deformations leads, at the end of drying, to a change in the sign of stresses. In the dried board, residual compressive stresses remain in the surface layers, while tensile stresses are present in the inner zone. For initial moisture content below 25 %, stress relaxation was not observed.

Fractal models and fractional-order differential equations.

In [33], a literature review on the mathematical modeling of non-isothermal moisture transport and viscoelastic deformation in capillary-porous materials with fractal structures was conducted. For describing unsteady processes in media with fractal structures, which exhibit: biological variability of rheological properties; structural heterogeneity; memory effects; self-organization; deterministic chaos; the mathematical apparatus of fractional-order differentiation was employed.

The Riemann-Liouville, Caputo, and Grünwald-Letnikov approaches, along with fractional integration operators, were applied.

Significant contributions to the development of mathematical models were made by B. Ugolev, G. Shubin, Ya. Sokolovskyy, I. Krechetov, and P. Biley.

The elastic and viscoelastic deformations have been extensively studied, whereas models incorporating fractal material structures remain underexplored.

Advances in mathematical models.

In [34], the mathematical model of non-isothermal moisture transport in capillary-porous drying materials was refined to account for their fractal structure and anisotropy of thermomechanical properties. The heat and mass transfer process during drying is described by a system of fractional-order partial differential equations based on the Riemann-Liouville formulation. The solution was implemented using the finite difference method.

The model accounts for:

1) elastic, viscoelastic, and residual deformations;
2) memory effects and self-organization;
3) the impact of wood species properties on moisture content variations;
4) the effect of fractal structure on the stress tensor distribution in wood.

Additionally, the Voigt, Maxwell, and Kelvin fractal models were considered.

The relationship between stress and strain components in wood drying, considering the fractal structure of the medium, is presented as a system of fractional-order differential equations. These equations were derived from the integral equations of viscoelasticity, which are based on the hereditary Boltzmann-Volterra theory.

To determine the criteria for selecting the relaxation kernel, the rheological behavior of wood and its fractal structure were taken into account. The kernel was chosen based on literature and experimental data. The solution was obtained using the predictor-corrector finite difference method. A two-dimensional viscoelastic deformation model of wood as a fractal medium was investigated under non-isothermal moisture transport conditions. The influence of drying process parameters on the distribution of temperature, moisture content, and stress-strain components was established.

5.3 DRYING PROCESS CONTROL AND OPTIMIZATION FOR ENERGY EFFICIENCY AND SUSTAINABILITY

The issue of controlling drying processes is addressed in many works, emphasizing the importance of precise process regulation to ensure efficient moisture removal while minimizing material degradation. Given the complex dynamic nature of drying, achieving optimal control requires the application of advanced mathematical models and systematic process analysis [35].

To simplify the study of complex dynamic systems, various structural transformations and equation modifications have been suggested, including:

Decomposition. Dividing the complex system into weakly coupled subsystems by selecting inverse connections, allowing the system to be managed through simpler, autonomous subsystems, each controlled independently by local regulators.

Aggregation. Combining smaller components into larger functional blocks to prevent excessive system complexity and order increase.

Transformation. Converting the system into a standardized form without changing the equation order, ensuring a more structured representation of the control scheme.

While these methodological approaches improve the structural representation of drying processes, a key challenge remains: achieving energy-efficient drying without compromising product quality. The drying process is energy-intensive, and unoptimized control strategies can lead to excessive energy consumption, material defects, and operational inefficiencies.

Thus, optimizing drying processes has become a crucial factor in advancing sustainable industrial practices. Strategies such as real-time process monitoring, adaptive control algorithms, and heat recovery systems contribute to energy savings and reduced environmental impact. Moreover, incorporating sustainability principles into drying system design ensures that industrial drying aligns with global energy efficiency goals and eco-friendly production standards.

Addressing drying optimization from an energy-saving and sustainability perspective requires an integrated approach, balancing technical performance, economic feasibility, and environmental responsibility.

3.1 GENERAL INFORMATION ON CONVECTIVE DRYING OF POROUS MATERIALS IN DRYING INSTALLATIONS

To proceed with the optimization of drying processes, it is essential to first understand the fundamentals of technological processes occurring in industrial drying facilities. In particular, a comprehensive knowledge of the types of drying equipment used and their specific purposes is required. The selection of appropriate drying methods and operating conditions depends on the properties of the material, the target moisture content, and the efficiency of heat and mass transfer mechanisms.

The optimal process parameters – such as environmental temperature T_s, air humidity in the drying chamber ϕ, and airflow velocity υ – must be carefully chosen considering the technological characteristics of the material being dried.

Moisture removal under heating is constrained by the maximum allowable temperature for a given material and the permissible gradient of its change over time. The control of temperature and humidity in drying chambers is achieved by regulating the dry-bulb T_c and wet-bulb T_m temperatures of the drying agent.

In steam-based chamber drying installations, the drying process follows the characteristics of dry-bulb T_c and wet-bulb T_m temperature changes.

In **Fig. 5.1**, the relative change in drying duration is plotted along the x-axis, representing the ratio of actual drying time τ to the standard drying cycle time τ_{nom} of 48 hours. The *y*-axis shows the relative value of the dry-bulb temperature, where a reference temperature of 120 °C is taken as the unit value.

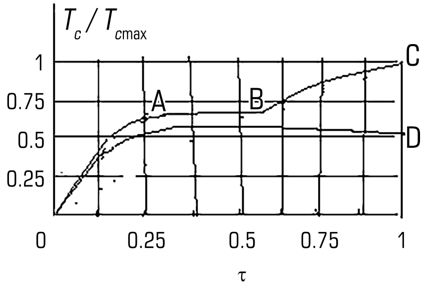

Fig. 5.1 Changes of T_c and T_m in the process of drying

During the drying process, three main stages can be distinguished:

1. Material heating stage.
2. Isothermal heating stage throughout the cross-section.
3. Falling drying rate stage.

The dry-bulb temperature varies at different stages of the drying process:

a) during the material heating stage (segment OA), the temperature increases at its maximum rate;

b) during the isothermal heating stage throughout the cross-section (segment AB), the temperature rise slows down, allowing temperature equalization across different layers of the material's thickness;

c) in the final stage (segment BC), dry-bulb temperature changes, and intensive moisture removal occurs along with changes in the drying potential.

In the first two stages (heating and isothermal heating), the moisture loss per unit time (drying rate) remains constant. As long as the moisture supplied to the surface exceeds the amount that the surrounding medium can absorb, the surface moisture content remains constant, meaning the material's surface remains moisture-saturated. Consequently, the moisture removal rate stays unchanged. Throughout this period, the surface temperature of the material remains stable and equals the adiabatic saturation temperature of the air (i.e., the wet-bulb temperature). The central part of the material, in contrast, heats up more slowly compared to the surface and reaches the wet-bulb temperature somewhat later in the drying process.

During the isothermal heating stage, the surface temperature and the temperature at the material's core remain unchanged, meaning that the temperature gradient inside the material is zero. At the same time, the temperature difference between the air and the material's surface remains constant. Under these conditions, with a constant heat transfer coefficient, the drying rate remains stable. This phase is referred to as the constant-rate drying period, characterized by an unchanging material temperature.

During this phase, moisture evaporates from the material's surface, as it is continuously supplied from the inner layers, keeping the surface moist. The material temperature closely approximates the wet-bulb temperature, and the drying rate reaches its maximum. This stage continues until the moisture content reaches a critical level, beyond which the surface temperature starts rising over time, and the drying rate begins to decline. The linear drying curve segment transitions into a curve that asymptotically approaches the equilibrium moisture content. The core temperature also rises, but its curve lags slightly behind the surface temperature curve. Consequently, a temperature gradient develops within the material, gradually diminishing until the equilibrium moisture content is reached, at which point the temperature gradient becomes zero. In this equilibrium state, moisture content no longer decreases, and the material temperature equals the air temperature.

The falling-rate drying period (segment BC for temperature increase, segment BD for drying rate decrease) is characterized by a gradual rise in material temperature and a decline in the drying rate.

Once all layers reach the same temperature, it becomes possible to lower the wet-bulb temperature by removing moisture-laden air from the drying chamber using an exhaust fan, increasing the dry-bulb temperature, and reducing steam humidification. This adjustment continues until the psychrometric difference (corresponding to a specific material moisture content) reaches a predefined value. The two-stage drying mode should be set according to material thickness, initial and final moisture content, and air velocity inside the chamber.

When temperature distribution is uniform, shrinkage does not induce critical stresses. However, shrinkage development is associated with the emergence of internal stresses. Preventing material cracking can be achieved by reducing tensile stresses through minimizing moisture gradients within the material's cross-section. This can be accomplished by softening the drying mode at the initial stage and applying thermal treatment in the middle and final stages.

In the two-stage drying process, during the constant-rate drying period, a high relative vapor pressure and a relatively low temperature are maintained. In the falling-rate drying period, the dry-bulb temperature increases to its maximum, while the relative vapor pressure decreases. The moisture content of the capillary-porous material at the transition from the first to the second stage should be equal to the fiber saturation point of the material.

For high-temperature drying modes, it is crucial to consider that the rate of moisture migration from the core to the surface is proportional to the moisture conductivity coefficient. The moisture conductivity coefficient increases with temperature, while the moisture content gradient increases as the relative humidity of the vapor decreases, due to the corresponding reduction in surface moisture. In high-speed, high-temperature hydrothermal treatment, controlling moisture gradients is critical for maintaining process rigidity, efficiency, and safety.

The rigidity of the drying regime is characterized by the magnitude of the psychrometric difference T_c–T_m and plays a critical role in high-temperature, high-speed drying. The rigidity must be adjusted continuously throughout the entire drying process when dealing with high initial moisture content and should be periodically regulated during low-temperature drying. The efficiency of the drying process is defined as the ratio of the normal drying time to the time spent in high-temperature mode. The safety of the process is determined by the ratio of the material's strength limit to the maximum stresses that develop under the given drying conditions.

One of the main obstacles to high-speed drying is cracking. The cause of cracks is the development of surface stress in the material, which exceeds the allowable limit. This stress state is created by unacceptable shrinkage, which occurs due to the uneven distribution of moisture content and temperature within the material. Cracking can be avoided by reducing tensile stresses through minimizing moisture gradients across the section. This can be achieved by softening the drying regime at the beginning and performing heat treatment in the middle and at the end of the process.

If to assume that local failure occurs in the elastic region under the action of normal tensile stresses, then in a plate of thickness $2L$, the moisture content gradient between the central and surface layers, given by $\frac{L}{3}\left(u_c - u_p\right)$, where u_c is the moisture content at the central surface and u_p is the moisture content at the outer surface, can serve as a criterion for determining moisture content based on critical normal stresses.

However, in the work of Voronov, it is noted that the calculated stresses exceed experimental values by a factor of 5 to 10 [35]. The author attributes this discrepancy to the inapplicability of Hooke's law, as local failure occurs in an elastoplastic region. It is also indicated that the cause of crack formation is shear stress, and the failure conditions reduce to ensuring that the intensity of shear stresses at a given point in the specimen reaches critical values, whereas tensile stresses alone cannot be the cause of local rupture. In real materials, local ruptures occur due to defects, weak points, and pre-existing cracks.

The process of material failure consists of two stages: local failure and complete failure. Crack formation occurs in the elastoplastic region under the influence of plastic deformations, which arise before the appearance of cracks and, at the moment of their formation, account for 60–80 % of the total deformation, depending on the moisture content of the material. The values of fracture-inducing stresses and ultimate failure stresses depend on the loading rate, increasing with the intensity of stresses by a factor of 2 or more. At high moisture content, the ultimate shear stress and the crack-inducing stress are approximately the same. As the moisture content decreases, the ultimate failure stress increases more than the crack-inducing stress [5].

The optimal drying regimes for capillary-porous materials are influenced by the material's shrinkage due to moisture changes. The shrinkage process varies across different materials. For example, in cement stone, shrinkage increases only when the moisture content drops below 30 %. Some materials, such as clay, begin to shrink immediately upon moisture reduction. Let's consider this effect in the case of wood. If the moisture content in a certain section falls below the hygroscopic limit, the fibers attempt to contract in size, but this is hindered by the fibers that still have a higher moisture content. As a result, internal stresses arise. The shrinking fibers, unable to contract, experience tensile stress, while adjacent fibers, influenced by the shrinking ones, are compressed.

As hygroscopic moisture is removed from the material, the shrinkage process gradually slows down. If a microscopic crack forms within the material, shrinkage may decelerate. If the internal cracking does not progress, shrinkage may resume at its previous rate and eventually stop after some time. This cessation occurs when the material reaches an average moisture content close to the equilibrium value corresponding to the given temperature and relative humidity of the drying agent. The shrinkage development law may follow various dependencies, such as an exponential decay. At the same time, it should be noted that wood is an anisotropic material, and shrinkage occurs below the fiber saturation point.

The dependence of the modulus of elasticity on moisture content is inversely proportional to moisture up to the fiber saturation point and can be approximated by straight lines with different slopes before and after this point. By maintaining the required surface moisture level, the desired values of permissible stresses can be ensured. The surface moisture is regulated by adjusting the moisture content of the drying agent.

According to [35], the moisture content distribution across the thickness of the material satisfies the expression $\frac{u_c - u_y}{u_c - u_p} = \left(\frac{y}{L}\right)^n$, where u_c, u_p, u_y are the moisture content values at the center, on the surface, and at a distance y from the center, respectively, and n is an exponent characterizing the steepness of the relative moisture distribution across the thickness. At the beginning of the drying process, $n \to \infty$, while at the end, $n \to 0$. Shrinkage follows an exponential dependence on time $\varepsilon = \varepsilon_k \left(1 - e^{-\tau/T}\right)$, where ε is the current shrinkage value, ε_k is the shrinkage at the end of the process, and T is the time constant.

At the beginning of the falling drying rate period, the moisture distribution across the thickness is parabolic $(n = 2)$.

For internal stresses in the layer at y, there is $\sigma_y = \frac{A}{3} u_y \left(2u_c - u_p - 3u_y\right)$. Further deepening of the evaporation zone is accounted for using a cosine-like distribution at $n = 1.5$:

$$\sigma_y = \frac{A}{2{,}5} u_y \left(1{,}5u_c - u_p - 2{,}5u_y\right).$$

At later stages, the distribution is assumed to follow a linear law $(n = 1)$: $\sigma_y = \frac{A}{2} u_y \left(u_c - u_p - 2u_y\right)$.

The coefficient A is determined by the material properties and the control system settings:

$$A = k\left[\varepsilon_k\left(1 - e^{-\tau/T}\right) + u_p\right].$$

Maintaining the desired surface moisture content ensures that the allowable stress limits are not exceeded. Thus, for a safe drying process, it is necessary to determine the optimal air velocity, relative humidity, drying agent temperature, and the timing of regulation phase transitions.

The change in moisture content with temperature variations inside the material over time depends on the interrelationship between internal moisture and heat transfer processes, as well as the heat and mass exchange at the material surface with the environment.

At low temperatures, thermodiffusion is minimal, and the resulting moisture flux coincides with the convective-diffusive vapor flux. During drying, moisture from the inner layers moves toward the surface, leading to a decrease in moisture not only at the surface but also in deeper regions. Evaporation occurs within the body at a specific zone or throughout the entire volume, depending on the pore size distribution density and the dispersion of pore sizes. In this case, moisture transport inside the material takes place in both liquid and vapor forms. The rate of moisture migration inside the material depends on the type of moisture binding.

Different approaches exist for optimizing the drying process. If the primary requirement is preventing cracks, the drying regime should be adjusted according to changes in the structural and mechanical properties of the material. If cracking occurs in the first drying period, the cracking criterion can be expressed as the relative moisture content gradient between the average moisture content $\bar{u}$ and the local moisture content u with respect to the initial moisture content $\bar{u}_0$:

$$K = \frac{\bar{u} - u}{\bar{u}_0}.$$

If cracking occurs on the surface in the first drying period, then $u = u_p$. For a parabolic moisture distribution: $K = \frac{2}{3}\frac{(u_c - u_p)}{\bar{u}_0}$, where $u_c - u_p$ is the difference in moisture content between the central and surface layers. The primary moisture transport criterion in the drying process is the Kirpichev criterion Ki', defined as the ratio of the surface moisture gradient ∇u_p to the initial moisture content $\bar{u}_0$, multiplied by the characteristic size of the material R. The obtained values of Ki' correspond to specific values of surface moisture content u_p and temperature t_p.

For the constant drying rate period with a parabolic moisture and temperature distribution, A. Lykov established that:

$$\frac{(u_c - u_p)}{\bar{u}_0} = \frac{1}{2}Ki' + \frac{t_p - t_c}{t_c}Pn,$$

where

$$Ki' = \frac{q'R}{a'\gamma_0\bar{u}_0}$$ is the Kirpichev criterion for moisture transfer,

and

$$Pn = \frac{\delta t_c}{u_0}$$ is the Postnov criterion.

Here, q' represents the evaporation rate, a' is the mass transfer potential conductivity coefficient $a' = \frac{\lambda'}{c'\gamma_0}$, where γ_0 is the skeleton density, R is half of the material thickness for a plate, and λ', c' are the moisture conductivity and moisture capacity, respectively.

Drying modes.

Under mild drying conditions, the temperature gradient in the first period is absent, and the relative moisture content gradient is directly proportional to the Kirpichev criterion. The criterion Ki' can be determined in various ways: by evaporation intensity q', by the moisture content difference $u_c - u_n$, by the surface moisture gradient, or by the decrease in moisture content over time:

$$Ki' = \frac{q'R}{a'\gamma_0\bar{u}_0} = \frac{2\left(u_c - u_p\right)}{\bar{u}_0} = -\frac{R\left(\nabla u\right)_p}{\bar{u}_0} = \frac{\left(\bar{u}_0 - \bar{u}\right)}{\bar{u}_0 Fo'},$$

where $\bar{u}$ is the average moisture content corresponding to the Fourier criterion:

$$Fo' = \frac{a'\tau}{R^2}$$

in the constant drying rate period. The maximum allowable Kirpichev criterion depends on the material's moisture content; as the moisture content decreases, the criterion increases. This criterion is directly proportional to the drying intensity q' and inversely proportional to the potential conductivity coefficient a'. Other parameters included in the criterion are the dry material density γ_0, initial moisture content u_0, and characteristic size R.

At low drying intensities q', it can be assumed to be equal to the evaporation rate of the liquid from a free surface. The evaporation rate is uniquely determined by the formula $q' = Nu'\frac{\lambda'}{l}\Delta p_i$, where λ' is the moisture conductivity coefficient. Heat and mass transfer coefficients under natural convection conditions are determined using Nesterov's formulas, which are provided later. Using these formulas, drying intensity is calculated at different air temperatures and humidity levels. During the constant drying rate period, the body temperature can be assumed equal to the wet-bulb temperature. Thus, given the parameters T_s and ϕ, the material's temperature and coefficient a' are uniquely determined.

With a graph of coefficient a' variations with temperature, a family of curves $Ki' = f\left(T_s\right)$ can be constructed for different values of ϕ at a constant air velocity and characteristic body size. If the maximum allowable Kirpichev criterion is known, and the dependence of Ki' on different moisture contents is plotted, an entire region of permissible drying modes is obtained, from which the mode with the highest drying intensity is selected. The drying apparatus should have minimal heat and electricity consumption. As the moisture content decreases, the maximum permissible criterion $Ki'_{\max}$ increases, and the range of allowable drying regimes expands. Therefore, optimal drying regimes should be stepwise, with drying intensity increasing as drying progresses.

Increasing air velocity reduces the range of permissible process parameters T_s and ϕ (the family of curves $Ki' = f\left(T_s\right)$ shifts upward), so at the beginning of the drying process, air velocities should be low. The air velocity is chosen based on a joint analysis of the allowable drying regime area with the calculated energy consumption, temperature, and humidity gradients for selected regimes in the given drying chamber.

At high air humidity levels (low drying intensity), heat transfer coefficients are close to those of heat exchange without mass transfer. The greater the sample length along the airflow direction, the lower the drying intensity.

During gentle drying modes, in the constant-rate period, the partial pressure of vapor near the surface of the material equals the saturated vapor pressure at the wet-bulb temperature. This value remains constant, even though the moisture content at the surface of the material gradually decreases to the maximum hygroscopic moisture content. The decrease in moisture content follows a complex curve that asymptotically approaches the equilibrium moisture level. At this stage, the material temperature is equal to the wet-bulb temperature.

In intensive drying modes, the heat and mass transfer patterns change. The temperature at any given point in the material, starting from the surface, gradually increases, while the decrease in moisture content at any point follows a linear law. This means that the drying rate remains constant, while the temperature increases, including at the surface layer. A temperature gradient is observed. The temperature near the surface of the material initially equals the wet-bulb temperature, but then continuously rises. By the end of the process, the air temperature and the material temperature equalize. Near the surface, the temperature distribution follows a linear law, which then transitions into a curve, asymptotically approaching the ambient temperature.

At the very surface, heat transfer occurs via molecular mechanisms (vapor diffusion in an inert gas). As the distance from the surface increases, molecular heat transfer transitions into molar (convective) transfer, which gradually intensifies. The thickness of the conditional boundary layer remains constant in the first period of drying but then increases approximately according to a linear law.

In the temperature range of 0–150 °C, when heating a product (e.g., bricks), hygroscopic moisture is removed, accompanied by a significant release of water vapor. The vapor pressure inside the product reaches high values even at 70 °C, increasing progressively as the temperature rises. If the rate of vapor generation inside the material exceeds the rate of vapor filtration through its thickness, the resulting internal pressure may lead to cracks and delamination. Furthermore, the surface of the material, having dried rapidly, continues to heat up significantly. Inside the material, the temperature quickly rises to 100 °C and remains at this level until complete moisture removal, creating significant temperature differences between the surface and the inner part of the product, leading to high stresses and crack formation.

Experiments show that if the final drying phase is carried out by increasing the gas flow rate with a moderate increase in temperature (50–80 °C per hour), the process occurs with high intensity, minimal temperature gradients across the material's thickness, and no damage to product quality. The temperature range of the drying process is critical: if it is narrow, a slow temperature rise and prolonged holding time are preferable. Holding the material at the maximum temperature ensures uniform temperature distribution throughout its thickness.

Cooling of the product after maximum temperature holding.

The cooling phase after holding the product at maximum temperature is just as critical in the drying process as the heating phase. In the initial stage of cooling, as the temperature decreases, materials undergo shrinkage and plastic deformations under minimal loads. During this phase, material cracking may occur. In each temperature range, the cooling intensity should be adjusted accordingly.

Let's consider, as an example, the intensification of chamber drying of lumber. The drying process is conducted under atmospheric pressure.

Evaporation occurs at any given temperature, but the higher the temperature, the more intense the evaporation. During evaporation, the molecules of liquid near the surface have higher velocity than others, and overcoming molecular cohesion forces, they escape into the surrounding environment. The process of evaporation is explained by the fact that the surface layer is heated slightly above the readings of the wet-bulb thermometer of a psychrometer placed in the surrounding environment. As a result, the vapor pressure of the liquid on the surface is higher than that in the drying agent. Boiling, on the other hand, occurs only at the saturation temperature. The vapor formed from boiling water is called wet saturated vapor. During boiling, the amount of water decreases until the last drop turns into vapor. Once the droplets have evaporated, the vapor becomes dry saturated. If the temperature of the dry saturated vapor increases without changing the pressure, it is referred to as superheated vapor.

Removing heat from superheated vapor leads to a decrease in its temperature and specific volume. Condensation of vapor occurs only when its temperature drops below the saturation temperature. These properties of vapor are widely used in drying technology.

Superheated steam, while expending part of its heat, can heat the material and evaporate moisture from it. As moisture evaporates from the material, the amount of vapor increases. To prevent a drop in pressure at the lower part of the chamber, a vapor outlet to the atmosphere or a heat exchanger must be installed. The saturation temperature of vapor depends only on pressure. Each specific vapor pressure corresponds to a saturation temperature. Knowing the water vapor pressure, it is easy to determine the temperature and vice versa. When saturated vapor is cooled, it condenses into water. During condensation, the saturated vapor releases all of its latent heat of vaporization. This heat is used in dryers for heating heat exchangers. The heat exchangers then transfer this energy to the drying agent, which, through convection, heats the material and facilitates moisture evaporation.

Methods of lumber drying using superheated steam.

Lumber drying using superheated steam can be achieved through the following methods:

1. Direct superheated steam supply: superheated steam from a boiler is introduced into a sealed drying chamber, where it is forcibly circulated through the stack of lumber. The used superheated steam, after mixing with the vaporized moisture from the wood, is expelled from the chamber. Closed-cycle drying with a vapor outlet pipe: A hermetically sealed chamber with a vapor outlet pipe is created. Inside the chamber, a heat exchanger with high thermal power and devices for circulating the drying agent are installed.

At the initial stage of drying, saturated steam is introduced into the chamber, which heats the wood and displaces air from the chamber. Simultaneously, the steam is circulated by fans through heat exchangers, where it becomes superheated. Once the introduced steam in the chamber turns superheated, it starts evaporating moisture from the wood, mixing with the vapor from the extracted moisture.

At this point, the steam supply to the chamber is stopped, as sufficient steam is generated from the moisture evaporated from the wood. The steam mixture is circulated by a fan through heat exchangers, increasing its degree of superheating, then passing through the lumber stack, and so on. Excess steam is removed through a vapor outlet pipe or directed to heat exchange systems.

2. The second method is more efficient than the first one because in hermetic chambers with vapor outlet pipes, heat losses associated with the intake of superheated steam from the boiler and its release into the atmosphere are eliminated.

At the beginning of the drying process, when the material has not yet heated up, the surface layers of the material, which are in contact with the hot chamber environment, have a higher temperature than the core. This creates a temperature gradient, which causes moisture movement toward lower temperatures, i.e., from the surface to the center. This phenomenon is known as thermo-hydroconductivity.

If wood is dried in an environment where the temperature exceeds 100 °C, an excess vapor-air mixture pressure may develop and persist inside the material for an extended period (compared to atmospheric pressure). This pressure induces a steady movement of water vapor (along with liquid water) from the center to the surface of the material, a process known as molar moisture transfer.

During drying, all driving forces act simultaneously, and their effects combine.

Drying concludes with the removal of moisture from the surface into the surrounding environment. The intensity of moisture removal depends on the difference in partial vapor pressures in the air layer above the wood surface and in the surrounding air, as well as on the velocity of the air flowing around the wood. The greater the difference in partial pressures and the air velocity, the more intense the moisture evaporation from the material's surface.

The heat and mass transfer criteria are expressed through the Nusselt criteria:

$$Nu = \frac{\alpha l}{\lambda_g} = \frac{ql}{\lambda_g \Delta t}; \quad Nu' = \frac{\alpha' l}{\lambda'_g} = \frac{q' l}{\lambda'_g \Delta p}, \tag{5.1}$$

where l is the characteristic linear dimension.

If the complex transfer mechanism is replaced by an equivalent molecular transfer, a conditional boundary layer of thickness δ is obtained. From experimental curves, the heat and mass transfer coefficients, as well as the Nusselt numbers, are determined using the following formulas:

$$\alpha = \frac{\lambda}{\delta_t}, \; \alpha' = \frac{\lambda'}{\delta_p}, \; Nu = \frac{l}{\delta_t}, \; Nu' = \frac{l}{\delta_p}. \tag{5.2}$$

By extending the moisture distribution lines of the air to the horizontal axis, the conditional depth of the evaporation surface ξ can be determined [5].

In *the first drying period*, the drying intensity remains constant despite the continuous deepening of the evaporation surface. This phenomenon is explained by the increase in the mass transfer coefficient λ' due to the displacement of the diffusion transfer mechanism of vapor in the boundary layer by the effusion mechanism in the surface layer of the material (evaporation zone).

The drying intensity in the first period is given by $q' = \frac{\lambda'_\phi}{\delta_\phi + \xi}\left(\phi - \phi_c\right)$.

In the first approximation, δ_φ is constant and greater than ξ. The increase in the denominator due to the growth of ξ is compensated by an increase in λ', thus maintaining a constant density of the drying flux. In the second drying period, δ_φ increases, leading to a reduction in drying intensity [36–40].

In the transition region from mild to intensive drying modes, the rate of evaporation front penetration remains constant during the first period, and evaporation occurs at a certain fixed depth, while the temperature distribution curves at different moments of the first period coincide with each other. The same applies to the humidity distribution curves of the air. In mild drying modes, during the first period, the evaporation front is close to the surface of the material. The Nusselt criteria, which characterize external heat and mass transfer, are inversely proportional to the thickness of the conditional boundary layer; therefore, they remain constant during the constant drying rate period and decrease over time during the falling drying rate period.

In intensive drying modes, the heat flux density can be determined as $q = r_k q' + \bar{c}\gamma_0 \frac{V}{F}\frac{d\bar{t}}{d\tau}$, where $\frac{V}{F}$ is the volume-to-surface ratio of the material, and r_k is the specific heat of evaporation.

Due to auxiliary expenditures when calculating heat flux density, the Nusselt criterion is determined by the conditional boundary layer thickness. Experimental studies have shown that in the first period, the Nusselt number remains constant, while in the second period, it decreases with decreasing moisture content. P. Lebedev obtained the empirical relationship $\frac{Nu}{Nu_n} = \left(\frac{u}{u_{kr}}\right)^n$, where u_{kr} is the critical moisture content, and Nu_n is the Nusselt number in the constant drying rate period, given by $Nu_n = A\left(\frac{T_c}{T_m}\right)^2 \left(\frac{T_u}{T_c}\right)^{0.4} Re^{0.5}$. For wood, $A = 0.5$, $n = 0.3$. Similar relationships hold for mass transfer: $\frac{Nu'}{Nu'_n} = \left(\frac{u}{u_{kr}}\right)^{n'}$, where the exponent n' is close to n. Thus, changes in heat and mass transfer follow the same pattern.

Calculating the Nusselt number Nu' using formulas (5.1) and the conditional boundary layer thickness shows that the Nusselt number Nu' calculated using formulas (5.1) in the first period is significantly higher than Nu' calculated based on the boundary layer thickness. The difference between them decreases as the moisture content decreases [5].

This difference is greater at higher drying intensities. This is explained by the vapor transfer mechanism through the evaporation zone. During evaporation, the evaporation front penetrates deeper into the material. Transfer within the evaporation zone occurs not only through diffusion but also effusion (molecular flow) if the capillary radius of the material is smaller than 10^{-5} cm and the pressure equals atmospheric pressure.

A distinguishing feature of molecular flow is the movement of gas from less heated regions of the capillary to more heated ones under the same pressure p. During drying, the surface of the material has a higher temperature compared to the evaporation zone surface. Thus, this temperature gradient accelerates molecular flow, as the driving potential of effusion flow is $\frac{p}{\sqrt{T}}$. In the case of diffusion transfer, the presence of a temperature gradient in the evaporation zone reduces transfer speed. If the material contains capillaries with radii greater than 10^{-5} cm, then a combined diffusion-effusion transport mechanism takes place.

In the presence of macroscopic capillaries, diffusion vapor transfer is complicated by thermal creep, which works as follows: if a temperature gradient exists along the walls of a macroscopic capillary, then circulation currents of moist gas arise. Gas near the capillary wall moves against the heat flow, while along the capillary axis, it moves with the heat flow. Since the capillaries near the evaporation surface have a lower temperature compared to the capillaries in the surface layer of the material, thermal creep facilitates vapor transfer through the evaporation zone.

From the surface of the material to the surrounding environment, vapor transfer occurs primarily by molar transport. The mass conductivity coefficient λ' in the evaporation zone – boundary layer near the material surface underline{is significantly greater than the molecular mass conductivity coefficient}. Therefore, the Nusselt numbers calculated using standard formulas are overestimated compared to those determined by the boundary layer thickness, which provides more accurate results. This new mass transfer mechanism affects both heat transfer and the hydrodynamics of heat exchange. The increase in the Nusselt number during the drying process is explained as follows:

– as the evaporation front penetrates deeper, vapor passes through this zone via a diffusion-effusion mechanism, complicated by thermal creep and the presence of a general pressure gradient. Upon exiting the surface layer of the material, the overall pressure gradient immediately relaxes, acting as a turbulence-inducing factor for the laminar flow of the surface layer of the vapor-gas mixture. As a result, heat exchange intensifies, leading to an increase in *Nu*. As moisture is removed, drying intensity decreases, and the heat transfer coefficient decreases, approaching the coefficient of pure heat transfer. The relationship between the criteria *Ki′* and *Nu′* is given by $Ki' = Nu' \cdot \frac{R}{l}\frac{\lambda_g}{a'\lambda_0\bar{u}_0}\left(p_{nm} - p_c\right)$. The criterion Ki' is an analogue of the Biot criterion $Bi = \frac{\alpha}{\lambda}R = Nu\frac{R}{l}\frac{\lambda_g}{\lambda}$ for heat transfer, where λ is the thermal conductivity coefficient of the material, and R is the characteristic size of the material (for an infinite plate – half its thickness) or the hydraulic radius $R_v = \frac{V}{S}$, which is the volume-to-surface ratio of the material.

Regulation of temperature and humidity in drying chambers is carried out by adjusting the temperature according to the dry-bulb T_c and wet-bulb T_m thermometers of the drying agent. The dry-bulb temperature takes different values at different stages of the drying process. During the heating stage of the material, the temperature changes at the maximum rate. In the stage of isothermal heating throughout the cross-section, the temperature increases slightly. Temperature equalization of individual layers across the material thickness occurs. At the final stage, changes in the dry-bulb temperature lead to intensive moisture removal and a shift in drying potential.

Evaporation of moisture from the wet-bulb thermometer surface occurs more intensively when the humidity of the drying agent is lower. Measuring humidity based on different readings of the dry and wet thermometers is reliable under the condition of hydrodynamic equilibrium, i.e., when $S\alpha\left(T_c - \tilde{T}_m\right) = CS\left(P_m - P_v\right)r$, where S is the evaporation surface of the wet-bulb thermometer, α is the heat transfer coefficient, C is the evaporation intensity coefficient of moisture from the wet-bulb thermometer surface, $P = 475$ mmHg is the total barometric pressure, P_v is the vapor pressure in the air, and $r = 595$ cal/kg is the latent heat of evaporation. From this relationship:

$P_v = P_m - A\left(T_c - \tilde{T}_m\right)$, where $A = \frac{\alpha}{Cr}$. By determining the partial pressure of vapor, the relative humidity of the drying agent can be found: $\varphi = \frac{P_v}{P_m}$.

The coefficient A is determined by the empirical formula:

$$A = 0.00001\left(65 + \frac{6.75}{\upsilon}\right),$$

where υ is the velocity of the vapor-air mixture in the chamber. Thus, the readings of the dry and wet thermometers determine the humidity and temperature of the drying agent, and information about its state is a necessary condition for high-quality drying. For the heating period, it is assumed that the wet-bulb temperature uniquely determines the humidity of the drying agent and, at constant T_c, does not depend on its temperature.

Drying with heated gas.

In many cases, drying of wet materials is carried out using heated gas. The drying process also takes place in drying chambers. In these devices, the drying mode changes over time. The drying mode is characterized by three parameters: the gas temperature t_c, humidity ϕ, and gas velocity υ. These parameters affect both the drying time and the quality of the material. Therefore, it is necessary to find such a mode that, with minimal drying time and the lowest heat consumption, provides the best technological properties of the material. To understand the impact of the drying mode on duration, it is necessary to obtain drying kinetics curves depending on the parameters characterizing the mode. From practice, it is known that increasing the drying agent temperature increases the drying intensity and critical moisture content. Increasing the temperature from 15 to 45 degrees results in a 2.5-fold increase in drying intensity in the first period. Increasing air humidity sharply reduces drying intensity and critical moisture content. For example, increasing air humidity from 0.177 to 0.758 decreases the intensity by approximately 4.5 times. Increasing air velocity increases intensity in the first period and has significantly less effect at the end of the process. The ratio between capillary moisture and adsorptively bound moisture significantly affects drying intensity in the second period and the critical moisture content, while it has little effect on intensity in the first period [5]. As the amount of capillary water increases, the critical moisture content decreases. Therefore, the greater the amount of bound water, the higher the critical moisture content. The critical moisture content characterizes the end of the period with a constant drying rate, after which the drying intensity decreases.

At high gas temperatures, in the first period, the drying rate is constant, and the surface temperature of the material continuously increases and significantly exceeds the wet-bulb temperature. The drying intensity equals the mass transfer intensity:

$$q = \alpha\left(t_c - t_{p.m}\right) = Nu\frac{\lambda_g}{l}\Delta t,$$

$$q' = \alpha'\left(p_{p.m} - p_c\right) = Nu'\frac{\lambda'_g}{l}\Delta p,$$

where q and q' are the heat and mass flux densities, respectively, $\Delta t = (t_c - t_{p.m})$ is the temperature difference between the gas and the body surface, $\Delta p = (p_{p.m} - p_c)$ is the partial pressure difference of vapor at the body surface and in the surrounding environment.

In the humidity range of 50–70 %, the following formulas are proposed for water evaporation from a free surface:

$$Nu = 0{,}46\mathrm{Re}^{0{,}53}, \quad Nu' = 0{,}63\mathrm{Re}^{0{,}52} \text{ at } 3\cdot 10^3 < \mathrm{Re} < 3\cdot 10^4.$$

The Reynolds number is defined as:

$$Re = \frac{\upsilon l}{\nu}.$$

Through the analysis of multiple heat and mass transfer experiments under forced convection of moist gas, the following relationships were established:

$$Nu = 2 + A\cdot \mathrm{Pr}^{0{,}33}\cdot \mathrm{Re}^{n}\cdot Gu^{m},$$

where constants are provided in **Table 5.1**.

Table 5.1 Constants for relationships heat and mass transfer

Re	***A***	***n***	***m***	***A'***	***n'***	***m'***
$1–2\cdot 10^2$	1.07	0.48	0.175	0.83	0.53	0.135
$3.15\cdot 10^3–2.2\cdot 10^4$	0.51	0.61	0.175	0.49	0.61	0.135
$2.2\cdot 10^4–3.15\cdot 10^5$	0.027	0.90	0.175	0.0248	0.90	0.135

For $Re > 200$, the term 2 is omitted, and the formula simplifies to:

$$Nu = A\cdot Pr^{0.33}\cdot Re^{n}\cdot Gu^{m}, \left(Pr = \frac{\nu}{a} = \frac{\mu}{a\gamma}\right).$$

Similarly, for mass transfer:

$$Nu' = 2 + A'\cdot (Pr')^{0.33}\cdot Re^{n'}\cdot Gu^{m'}, \left(Pr' = \frac{\nu}{D}\right).$$

Here υ is the viscosity coefficient, and D is the diffusion coefficient. For an ideal gas, $\mathrm{Pr} = Pr' = 1$, for dry air $\mathrm{Pr} = 0.73$, and for vapor transport in an inert gas $Pr' = 0.75$.

Under conditions of natural convection:

$$Nu = 4(\mathrm{Pr}\cdot Ar)^{0.108}, \text{ for } (\mathrm{Pr}\cdot Ar) = 3\cdot 10^{6} - 2\cdot 10^{8},$$

$$Nu' = 4(Pr'\cdot Ar)^{0.248}, \text{ for } (Pr'\cdot Ar) = 1\cdot 10^{4} - 3\cdot 10^{8}.$$

When calculating these criteria, the characteristic size is taken as the side of a square equivalent to the liquid surface area $Ar = \frac{l^3 g}{v^2}\frac{\Delta\gamma}{\gamma_p}$.

Here, l is the length of the surface in the direction of the flow, g is the acceleration due to gravity (m/s^2), and $\Delta\gamma = \gamma_p - \gamma_c$ is the difference in density between the moist gas at the liquid surface and the bulk gas flow. In heat transfer, this density difference is replaced by the temperature difference and is known as the Grashof number criterion.

In all these equations, the thermal conductivity of the humid gas is calculated using $\lambda = \lambda_0 + 0.0041\varphi$, where λ_0 is the thermal conductivity of the dry gas. The mass transfer coefficient (diffusion coefficient relative to partial pressure differences) is calculated as $\lambda' = a_0' \frac{M_v T}{R T_0^2}\left(\frac{P_0}{p_b}\right)$, where a_0' is the diffusion coefficient under normal conditions. For water vapor, $a_0' = 0.079$ m^2/h, M_v = 0.018 kg/mol is the molecular weight of vapor, P_0 = 760 mmHg is the total barometric pressure, and T_0 = 273.2 K is the absolute temperature under normal conditions. The universal gas constant is R = 0.06237 m^3 mmHg/K mol, and the average absolute boundary layer temperature is $T = 273 + \frac{1}{2}(t_c + t_p)$, where p_b is the partial pressure of dry vapor in mmHg.

Wood drying process.

Initially, drying proceeds rapidly and slows down towards the end. The first stage involves heating the wood in the chamber. The moisture in the wood does not decrease; instead, it slightly increases due to condensation of atmospheric moisture on the cold wood surface.

The second stage involves drying from high initial moisture content w_0 to the critical moisture content w_{kr}, which is slightly higher than the hygroscopic boundary (which is 30 %). During this stage, free moisture is removed from the wood, making this phase the most intense.

The third stage involves drying from critical moisture to the desired final moisture content. Here, bound moisture is removed, and the process is slower than in the second stage.

Stresses developing in wood.

During drying, moisture is initially removed from the surface, leading to an uneven distribution of moisture throughout the volume. When the moisture content falls below the hygroscopic limit, shrinkage begins. (The property of wood to reduce its linear dimensions and volume when bound water is removed (at a moisture content below 30 %) is called shrinkage.) This leads to the formation of tensile moisture stresses in the surface layers, which can result in external cracks. To prevent this, drying should be slowed down by creating a highly saturated steam environment in the chamber (this is known as moisture-heat treatment).

As the moisture gradient across the thickness decreases, the stresses also decrease. When the moisture content of the inner layers of the wood falls below the hygroscopic limit, the inner part begins to shrink, while the outer, being dry and in tension, resists the shrinkage of the inner layer. This leads to the development of tensile stresses in the inner layer. If these tensile stresses continue to develop, internal cracks will form. Internal stresses can be reduced through thermal-humidity treatment of the wood.

Low-temperature and high-temperature drying processes.

Depending on the temperature level, the drying process can be classified as low-temperature or high-temperature.

Low-temperature drying occurs when the wood temperature remains below the boiling point of water at the given pressure (< 100 °C).

High-temperature drying occurs when the temperature in the central zones exceeds 100 °C. In this case, vaporization characteristics differ at different temperature levels.

For the high-temperature process, it is necessary not only for the surrounding medium to exceed 100 °C but also for the material itself to reach this temperature while still containing free water capable of boiling. An example of such a process is the drying of wood with an initial moisture content higher than the hygroscopic limit in a superheated steam environment under atmospheric pressure. A key feature of high-temperature drying is the intense transfer of moisture in the form of steam from the central zones to the peripheral ones. There is also an intermediate transition process between high- and low-temperature drying.

Drying chamber air circulation and types of chambers.

The circulation of the drying agent can be natural or forced, one-way or reversible. It is achieved using fans inside the chamber or through ejector nozzles, in which case the chambers are called ejection chambers.

Drying chambers are classified based on the drying agent:

– air chambers (where drying is done with heated air);

– superheated gas chambers;

– gas chambers, where the drying agents are combustion gases or natural gases mixed with humid air.

Based on operational principles, drying chambers can be:

– batch (periodic) operation: the material is loaded into the chamber in a full batch. If the chamber operates cyclically, the process consists of loading, drying, and unloading;

– continuous operation: the drying process does not stop for loading and unloading. The material moves continuously from the loading end to the unloading end of the chamber. With each unloading cycle, the stacks of material shift forward by the length of one stack [3].

CONCLUSIONS

To calculate the optimal drying regime, which is determined by technological changes during the drying process, it is crucial to study the laws of moisture transfer to effectively control it. One possible way to manage the moisture transfer mechanism is by influencing the processes of diffusion and thermodiffusion.

When drying with heated air, the total moisture flux equals the difference in moisture gradients, which are determined by the gradients of moisture content and temperature $q_m = = a_m \left|\frac{\Delta u}{\Delta x}\right| - a_m \delta \left|\frac{\Delta t}{\Delta x}\right|$. Under the influence of a temperature gradient, moisture moves inside the material. The moisture flux directed toward the material surface decreases due to the thermodiffusion-induced moisture flux. The temperature gradient acts as a barrier to the movement of liquid from the central layers to the surface. At a constant drying intensity, conditions are created that facilitate the evaporation of liquid within the material. Thermodiffusion reduces the moisture gradient, slows down the movement of liquid moisture, and decreases the amount of water-soluble substances on the material surface. Changes in the magnitude and direction of the temperature gradient alter the conditions for moisture movement and the transfer of dissolved substances, leading to changes in the physicochemical properties of the material.

In the case of drying with heated air, the temperature gradient in the material leads to a significant moisture content gradient, generating high stresses that can cause cracking. By accelerating heating and cooling from the surface, it is possible to achieve values of the Postnov criterion $Pn = \frac{\delta \Delta t}{\Delta u}$, where δ is the thermogradient coefficient, Δt is the temperature difference, and Δu is the moisture content difference, at which the moisture content distribution will be close to uniform.

Under these conditions, moisture and temperature stresses in the material do not develop, allowing for fast drying without cracks.

The method of heat transfer to the material affects the substance and heat transfer mechanisms during thermal processing. In the steam-thermal method, saturated steam is used as the heat carrier. Heat is transferred to the material via convection from the steam-air environment. This creates a significant temperature gradient in the material, resulting in internal stresses. Since the material temperature is lower than that of the steam-air environment, a condensate film forms on the surface. According to the law of moisture-thermal conductivity, moisture migrates from the surface layers to the central ones, leading to moisture absorption by the material. Over time, developed reaction hydration contributes to the material's temperature exceeding that of the surrounding medium. Consequently, intense moisture evaporation occurs with a significant moisture content gradient, forming directed porosity within the material.

An important heat transfer method involves the interaction of an alternating magnetic field with ferromagnetic elements. The wet material, along with ferromagnetic heat-generating elements, is placed in an electromagnetic coil field powered by industrial-frequency current. The ferromagnetic materials heat up and transfer heat to the wet material. Depending on the material properties, the heat transfer method is selected, and it can be adjusted based on the technological scheme for placing ferromagnetic elements (in volume, in a layer, stack, or mass). This method prevents high stresses and deformations in the material, ensuring drying without warping or internal cracks.

During thermal treatment in an electromagnetic field, heat is conducted to the material from the formwork and reinforcement. This creates a minimal temperature gradient in the material. In this case, the surface temperature is higher than that of the environment, and evaporation occurs with a slight moisture content gradient. Such a thermal treatment method increases the number of closed pores compared to steaming, improving material quality. Using the principles of diffusion and thermodiffusion, the substance transfer mechanism can be controlled. Since diffusion is determined by the diffusion coefficient and thermodiffusion by the thermodiffusion coefficient, establishing the dependence of these coefficients on moisture content and temperature is crucial for regulating the transfer coefficient.

REFERENCES

1. Nigmatulin, R. I. (1978). Osnovy mekhaniki geterogennykh sred. Moscow: Nauka, 336.
2. Gamaiunov, S. N., Misnikov, O. S. (1988). Usadochnye iavleniia pri sushke prirodnykh organomineralnykh dispersii. Inzhenerno-fizicheskii zhurnal, 71 (2), 233–236.
3. Mushtaev, V. I.; Planovskii, A. N. (Ed.) (1971). Osnovnye teoreticheskie polozheniia konvektivnoi sushki i utochnennyi metod rascheta sushilnykh apparatov. Moscow: MIKhM, 81.
4. Mushtaev, V. I., Ulianov, V. M. (1988). Sushka dispersnykh materialov. Moscow: Khimiia, 352.
5. Likov, A. V. (1968). Teoriia sushki. Moscow: Energiia, 472.
6. Sazhin, B. S. (1984). Osnovy tekhniki sushki. Moscow: Khimiia, 320.
7. Laitfud, U. (1977). Iavleniia perenosa v zhivykh sistemakh. Moscow: Mir, 210.
8. Tutova, E. G., Grinchik, N. N. (1984). Mekhanizm massoperenosa pri obezvozhivanii slozhnykh-biologicheskikh sistem. Teplomassoobmen – 6. Vol. 7. Minsk: ITMO AN BSSR, 25–28.
9. Grinchik, N. N. (1991). Protcessy perenosa v poristykh sredakh, elektrolitakh i membranakh. Minsk: ITMO im. A. V. Likova AN BSSR, 251.
10. Lutcik, L. P., Litevchuk, D. P. (1984). Vliianie porovoi struktury na pronitcaemost kapilliarno-poristykh tel. Teplomassoobmen – 6. Vol. 7. Minsk: ITMO AN BSSR, 74–77.
11. Likov, A. V. (1970). Metody resheniia nelineinykh uravnenii nestatcionarnoi teploprovodnosti. Izv. AN SSSR, Energetika i transport, 25, 109.
12. Zhuravleva, V. P. (1972). Masso-teploperenos pri termoobrabotke i sushke kapilliarno-poristykh stroitelnykh materialov. Minsk, 189.

13. Zhuravleva, V. P. (1971). Issledovanie protcessa obrazovaniia dispersnykh struktur. Minsk, 5, 35–40.
14. Kutc, P. S., Grinchik, N. N. (1984). Teplo- i massoperenos v kapilliarno-poristykh telakh pri intensivnom paroobrazovanii s uchetom dvizheniia fronta ispareniia. Teplomassoobmen – 6. Vol. 7. Minsk: ITMO AN BSSR, 93–96.
15. Lutcik, P. P. (1985). Uravneniia teorii sushki deformiruemykh tverdykh tel. Promyshlennaia teplotekhnika, 7 (6), 20.
16. Lutcik, P. P. (1984). Massotermicheskoe deformirovanie kapilliarno-poristykh kolloidnykh tel v protcessakh sushki. Teplomassoobmen – VII. Vol. 6. Minsk: ITMO AN BSSR, 90.
17. Haivas, B. I. (2010). Pro opys lokalnoho stanu kapiliarno-porystykh ta shchilno upakovanykh zernystykh materialiv v protsesi sushinnia. Chastyna I. Modeliuvannia ta informatsiini tekhnolohii. Kyiv: Instytut problem modeliuvannia v enerhetytsi im. H.Ie. Pukhova NAN Ukrainy, 57, 95–104.
18. Haivas, B. I. (2010). Kliuchova systema rivnian dlia doslidzhennia protsesu sushinnia porystykh til. Chastyna 2. Modeliuvannia ta informatsiini tekhnolohii. Kyiv: Instytut problem modeliuvannia v enerhetytsi im. H. Ye. Pukhova NAN Ukrainy, 58, 116–125.
19. Haivas, B. (2010). Matematychne modeliuvannia konvektyvnoho sushinnia materialiv z urakhuvanniam mekhanotermodyfuziinykh protsesiv. Fizyko-matematychne modeliuvannia ta informatsiini tekhnolohii. Lviv: TsMM IPPMM im. Ya.S. Pidstryhacha NAN Ukrainy, 12, 9–37.
20. Hayvas, B., Torskyy, A., Chapla, Y. (2012). On an approach to solution of problems of porous bodies drying. Fizyko-matematychne modeliuvannia ta informatsiini tekhnolohii. Lviv: TsMM IPPMM im. Ya.S. Pidstryhacha NAN Ukrainy, 16, 42–51.
21. Haivas, B., Boretska, I. (2011). Vplyv rezhymu sushylnoho ahenta na osushennia porystykh til. Kompiuterni tekhnolohii drukarstva, 26, 231–240.
22. Romankov, P. G., Rashkovskaia, N. B. (1968). Sushka vo vzveshennom sostoianii. Lviv: Khimiia, 360.
23. Teplitckii, Iu. S. (2002). Diagramma fazovogo sostoianiia dispersnoi sistemy s voskhodiashchim potokom gaza. Inzhenerno-fizicheskii zhurnal, 75 (1), 117–121.
24. Kalenderian, V. A., Karnaraki, V. V. (1982). Teploobmen i sushka v dvizhushchemsia plotnom sloe. Kyiv: Vishcha shkola, 160.
25. Buevich, Iu. A., Bugkov, V. V. (1978). O sluchainykh pulsatciiakh v grubodispersnom psevdoozhizhennom sloe. Inzhenerno-fizicheskii zhurnal, 35 (6), 1089–1097.
26. Buevich, Iu. A., Korolev, V. N. (1991). Obtekanie tel i vneshnii teploobmen v psevdoozhizhennom sloe. Sverdlovsk: Izd. Uralskogo universiteta, 188.
27. Nagornov, S. A. (2002). Upravlenie protcessami perenosa teploty v neodnorodnykh psevdoozhizhennykh i vibrotcirkuliatcionnykh sredakh. Tambov: GNU VIITKN, 101.
28. Razumov, I. M. (1972). Psevdoozhizhenie i pnevmotransport sypuchikh materialov. Moscow: Khimiia, 240.

29. Antonishin, N. V., Geller, L. A., Ivaniutenko, I. I. (1982). Teploperedacha v psevdoturbulentnom sloe dispersnogo materiala. Inzhenerno-fizicheskii zhurnal, 43 (3), 360–364.
30. Kheifetc, L. I., Neimark, F. M. (1982). Mnogofaznye protcessy v poristykh sredakh. Moscow: Khimiia, 320.
31. Akulich, P. V., Milittcer, K. U. (1998). Modelirovanie neizotermicheskogo vlagoperenosa i napriazhenii v drevesine pri sushke. Inzhenerno-fizicheskii zhurnal, 71 (3), 404–411.
32. Shubin, G.S. (1985). Sushka i teplovaia obrabotka drevesiny. [Extended abstract of Doctoral thesis].
33. Shimanskii, V. M. (2015). Matematichne modeliuvannia neizotermichnogo vologoperenesennia ta v'iazkopruzhnogo deformuvannia u seredovishchakh z fraktalnoiu strukturoiu. [Extended abstract of PhD thesis].
34. Sokolovskii, Ia. I., Shimanskii, V. M. (2011). Dvovimirna matematichna model vologoperenosuu kapiliarno-poristikh materialakh z fraktalnoiu strukturoiu. Naukovii visnik NLTU Ukraini, 21 (2), 341–348.
35. Voronov, V. G., Mikhailetckii, Z. N. (1982). Avtomaticheskoe upravlenie protcessami sushki. Kyiv: Tekhnika, 109.
36. Gayvas, B., Markovych, B., Dmytruk, A., Havran, M., Dmytruk, V. (2024). The methods of optimization and regulation of the convective drying process of materials in drying installations. Mathematical Modeling and Computing, 11 (2), 546–554. https://doi.org/10.23939/mmc2024.02.546
37. Dmytruk, A. (2024). Modeling mass transfer processes in multicomponent capillary-porous bodies under mixed boundary conditions. Mathematical Modeling and Computing, 11 (4), 978–986. https://doi.org/10.23939/mmc2024.04.978
38. Sokolovskyy, Y., Drozd, K., Samotii, T., Boretska, I. (2024). Fractional-Order Modeling of Heat and Moisture Transfer in Anisotropic Materials Using a Physics-Informed Neural Network. Materials, 17 (19), 4753. https://doi.org/10.3390/ma17194753
39. Decker, Ž., Tretjakovas, J., Drozd, K., Rudzinskas, V., Walczak, M., Kilikevičius, A. et al. (2023). Material's Strength Analysis of the Coupling Node of Axle of the Truck Trailer. Materials, 16(9), 3399. https://doi.org/10.3390/ma16093399
40. Gayvas, B. I., Markovych, B. M., Dmytruk, A. A., Havran, M. V., Dmytruk, V. A. (2023). Numerical modeling of heat and mass transfer processes in a capillary-porous body during contact drying. Mathematical Modeling and Computing, 10 (2), 387–399. https://doi.org/10.23939/mmc2023.02.387